Arresting Amyloid with Coulomb's Law: Acetylation of ALS-Linked SOD1 by Aspirin Impedes Aggregation.

Alireza Abdolvahabi[a], Yunhua Shi[a], Nicholas R. Rhodes[a], Nathan P. Cook[b], Angel A. Marti[b,c], Bryan F. Shaw[a*]

[a]Department of Chemistry and Biochemistry, Baylor University, Waco, TX 76798-7348
[b]Department of Chemistry, and [c]Department of Bioengineering, Rice University, Houston, TX 77005

SUPPORTING MATERIAL

SUPPORTING MATERIALS AND METHODS

Acetylation of native apo-SOD1 with aspirin:

As briefly described in the main text, successive acetylation of lysine residues in WT and ALS-variant native apo-SOD1 by aspirin was performed by dissolving acetylsalicylic acid crystalline directly in solutions of apo-SOD1 (5 μM SOD1 dimer) in 100 mM HEPBS (N-2-hydroxyethyl piperazine-N′-4-butanesulfonic acid), pH 9.0. The final concentration of aspirin was 25 mM, 50 mM, and 150 mM. The solutions of apo-SOD1 and acetylsalicylic acid were stirred for 48 hr at 4 °C. Throughout the acetylation and hydrolysis reactions, both of which produce acetic acid, the pH was maintained at pH 8-9 by addition of 3 M KOH. As a control, solutions of unacetylated apo-SOD1 were incubated alongside acetylated proteins, in the identical HEPBS buffer as the acetylated proteins, wherein no acetylsalicylic acid was added. Thus, the unmodified apo-SOD1 proteins were processed under the exact same solution conditions as the acetylated proteins. Reaction by-products (i.e., acetic acid and salicylic acid) and unreacted acetylsalicylic acid were removed with centrifugal filtration devices (5 kDa molecular weight cut-off, Corning® Spin-X® UF). Centrifugal filtration was also used to transfer proteins into an "aggregation buffer" consisting of 10 mM potassium phosphate, 5 mM EDTA, pH 7.4 (for carrying out thioflavin-T fluorescence amyloid assays). Centrifugal filtration consisted of diluting protein solutions (ten-fold) into the aggregation buffer and concentrating ten-fold (typically from 25 mL to 2.5 mL). This ten-fold concentration and dilution cycle was performed seven times for each sample.

Acetylation of fibrillar SOD1 with aspirin:

In order to prepare peracetylated apo-SOD1 fibrils (i.e., acetylating SOD1 after fibrillization), we combined 1.62 g of acetylsalicylic acid to 3.0 mL of unacetylated fibril homogenate (containing ~ 240 μM SOD1 polypeptide). The fibrils were prepared from 3.0 mL of 60 μM apo-SOD1 monomer as described for ThT fluorescence assays. Negative control samples contained the same amount of fibrils without the addition of aspirin. During the course of acetylation, the pH of the solution of acetylated fibrils drops as acetic acid is produced from hydrolysis of aspirin. The pH of the reaction was therefore maintained between pH ~ 8-9 by addition of 12 M KOH. Both acetylated and control samples were gently stirred with a stir bar (at room temperature, ~ 23 °C) during the course of reaction. In order to ensure that total protein concentrations were identical for control and acetylated samples, an aliquot of aggregation buffer (10 mM potassium phosphate, 5 mM EDTA, pH 7.4) was added to the control sample to keep its volume equal to that of the acetylated sample (the volume of which increased over time as KOH was added). After dissolution of aspirin (~ 1 hr), both acetylated and control samples were gently stirred for an additional 48 hr at 4 °C, pH 9.5. The pH of the acetylated sample was maintained at ~ 9.5 by periodic addition of 3 M KOH.

After 48 hr, the acetylated sample underwent 10 cycles of washing with aggregation buffer (10 mM potassium phosphate, 5 mM EDTA, pH 7.4) to remove salicylic acid, acetic acid, and any unreacted acetylsalicylic acid or non-aggregated SOD1. The washing process was as follows: centrifugation at 16,200 × g (4 °C), followed by removal of supernatant, addition of fresh buffer to the pellet, and additional centrifugation. The removal of salicylic acid was monitored with UV-Vis spectrophotometry (UV-2550, Shimadzu Corp., Kyoto, Japan) by the diminishing absorbance at 280 nm, i.e., salicylic acid absorbs strongly at 280 nm (1). Washed

samples were then separated into either 200 µL or 500 µL aliquots to be used for thermal stability assays and mass spectrometry.

Capillary electrophoresis (CE):

CE experiments were performed on a Beckman Coulter Inc. P/ACE electrophoresis instrument, in order to confirm the acetylation of apo-SOD1 as well as determining the number of acetylated lysine residues, as previously described (2). Potassium phosphate buffer was used as the running buffer (10 mM potassium phosphate, pH 7.4). Dimethylformamide (DMF) was added to each solution of protein (immediately prior to injection) as a neutral marker of electroosmotic flow, as previously described (2).

Differential scanning calorimetry:

The effect of acetylation on the thermostability of apo-SOD1 was measured with differential scanning calorimetry (DSC). Calorimetry was performed on acetylated apo-SOD1 (without the addition of reducing agent) in potassium phosphate buffer (10 mM potassium phosphate, pH 7.4, [SOD1] = 2 mg/mL) using a Microcal LLC VP-DSC (Microcal/GE-Healthcare), as previously described (3). The melting transition temperature (T_m) that was reported for each protein was an average of three separate measurements.

Hydrogen/Deuterium exchange:

The rate of amide hydrogen/deuterium exchange (HDX) of apo-SOD1$^{S\text{-}S}$ was measured with ESI-MS as previously described (4) using a LTQ LX/Orbitrap Discovery LC/MS (Thermo Scientific). Samples of each acetylated apo-SOD1 protein were concentrated in potassium phosphate buffer (100 mM phosphate, pH 7.4). Each sample was diluted 1:10 into D_2O and aliquots were then measured at three time points: 3 min, 60 min, and 120 min after dilution (seven replicates each). This exchange reaction was performed at room temperature and the samples were flash frozen at each time point. At the end of the H/D exchange experiment, the remaining solution was divided into seven aliquots for the purpose of SOD1 denaturation (perdeuteration) and measuring the extent of deuterium/hydrogen back-exchange. The specific temperatures that were used to perdeuterate WT, D90A, and A4V apo-SOD1 scaled with their relative thermostability and were 50 °C (for WT and D90A) and 37 °C (for A4V). The perdeuterated samples were then flash frozen in liquid nitrogen. All deuterated samples were then rapidly thawed (individually), and diluted 1:20 with ice-chilled formic acid (0.1%, in H_2O) and measured with ESI-MS. The ESI-MS was equipped with a desalting column (submerged in ice to minimize back-exchange) that was attached to an external, free standing Rheodyne injector that was also submerged in ice. Protonated solvents were used for ESI-MS, as previously described (4).

Transmission electron microscopy:

To determine whether aggregates of acetylated and unacetylated native WT and ALS-variant apo-SOD1 were fibrillar in nature, and to assess morphological characteristics of fibrils (e.g., fibril diameter and length), we analyzed aggregated solutions with Transmission Electron

Microscopy (TEM) at the end of the 10-day aggregation assay, as previously described (3). Imaging with TEM was also used to determine whether non-sedimentable oligomers remained in the supernatant of melted fibrils after completion of the thermal stability assays and filtration with a 0.2 µm filter (thermal stability assays are described in the main text). All samples were imaged using a JEOL 1230 High Contrast Transmission Electron Microscope operating at 80 kV and samples were prepared as previously described (3).

Liquid chromatography and mass spectrometry:

The number of acetylated amino acid residues in apo-SOD1 was confirmed with electrospray ionization-mass spectrometry (ESI-MS) using a LTQ LX/Orbitrap Discovery LC/MS (Thermo Scientific). In order to determine the identity of the residues that were acetylated in native (non-fibrillar) SOD1, we sequenced acetylated SOD1 with ESI-MS/MS after proteolysis with trypsin (Trypsin Gold, Mass Spectrometry Grade, Promega Corp.) and porcine pepsin (Sigma-Aldrich®). Trypsin and pepsin proteolysis was performed on separate aliquots of apo-SOD1, and not in tandem. Aliquots of the proteolytic digest of acetylated apo-SOD1 (10 µL, [SOD1] = 1 mg/mL) were loaded onto a C-18 Zorbax column using the same water/acetonitrile gradient described previously (2). All MS/MS spectra were analyzed using Proteome Discoverer 1.3 (Sequest 1.2) from Thermo Scientific.

Thioflavin-T aggregation assays:

Assays were performed at pH 7.4, 37 °C, in a 96-well black polystyrene plate with a Thermo Scientific Fluoroskan Ascent 2.5 Fluorescence spectrophotometer; fibrillization was initiated by the addition of a Teflon® bead to each solution, in each well of the microplate. We performed 18 replicates of ThT assays for each of the three apo-SOD1 proteins and the four sets of acetylated derivatives, in the presence and absence of 100 mM NaCl, a total of 432 separate assays. In order to extract the kinetic parameters of each aggregation assay, a sigmoidal function (Equation (1) and Fig. S2) was fit to plots of fluorescence vs. time (each plot consisted of 1000 scans for each well) using SigmaPlot™, version 11.0 (Systat Software Inc., Chicago, IL, USA).

$$f = y_0 + \frac{a}{1+e^{-\left[\frac{(x-x_0)}{b}\right]}} \qquad (1)$$

In Equation (1), f = fluorescence intensity (arbitrary units; a.u.); a = maximum emission intensity; y_0 = starting emission intensity; x = time in hours; and x_0 = time of 1/2 maximum emission intensity. As a template, we show a graphical representation of these parameters within a typical sigmoidal function (Fig. S2). The two most important parameters (for quantifying the rate of aggregation) are "x_0 -$2b$", which we refer to as "lag time" and "b", which is equal to the reciprocal rate constant of fibril propagation (1/k), where k represents the fibrillization rate constant. We refer to "b" as "reciprocal rate constant of propagation" or simply "inverse propagation constant". Kinetic parameters were extracted from sigmoidal fits of all 18 replicate plots for each acetylated and unacetylated apo-SOD1 protein. Average kinetic parameters were reported as mean values and error values were reported as standard error of the mean (SEM). The statistical significance of measured differences in the kinetic parameters of aggregation between acetylated and unacetylated proteins was determined with an unpaired Student's t-test,

using GraphPad Prism® software (GraphPad Inc., La Jolla, CA, USA). A threshold of significance of $p < 0.05^{*}$ (at a 95 % confidence interval) was used to establish the statistical significance of differences between the mean kinetic parameters of fibrillization of acetylated and unacetylated proteins.

The amount of apo-SOD1 that remained in solution at the end of ~ 10-day aggregation assay was determined with SDS-PAGE in order to ensure that aggregation proceeded to completion, without any remaining soluble SOD1. For this analysis, solutions of aggregated apo-SOD1 were pelleted with centrifugation at 16200 × g for ten minutes (on a Fisher Scientific™ accuSpin™ Micro 17/Micro 17R microcentrifuge) and SDS-PAGE was performed on the resulting supernatant, as previously described (3).

Size-exclusion chromatography and native polyacrylamide gel electrophoresis:

In order to characterize the non-sedimentable oligomers of apo-SOD1 after thermal defibrillization assays, we performed size-exclusion chromatography and native PAGE. Prior to SE-LC, the supernatant of the heated samples were immediately combined with pure (14.3 M) β-mercaptoethanol (β-ME) in a 60:1 (v/v) ratio (sample:β-ME) to prevent the formation of disulfide cross-links. Defibrillized solutions (300 µL) were injected into a 25 cm Zorbax Bio Series G-250 column (Agilent Technologies, Santa Clara, CA, USA); internal diameter = 4.6 mm; resolving range = 4-400 kDa. The aggregation buffer (10 mM potassium phosphate, 5 mM EDTA, pH 7.4) was used as a running buffer with a flow rate of 0.2 mL/min. The total run time was 40 minutes and the void volume (V_o) of the column was calculated to be 1.38 mL. Eluted species were detected at 280 nm using a photodiode array (PDA) detector. In order to approximate the molecular weight of the thermally defibrillized apo-SOD1 proteins that were generated during thermal melting experiments, we generated a calibration curve using a mixture of 5 different proteins with known molecular weights: phosphorylase b, lactate dehydrogenase (tetramer), albumin, WT apo-SOD1 (dimer), and ubiquitin. The concentration of each protein in the standard was 50 µM, except ubiquitin, which was prepared at 100 µM, because of its low absorbance at 280 nm.

For native PAGE experiments, defibrillized samples (containing β-ME) and native WT apo-SOD1 (dimer, used as a control) were diluted two-fold with native 2X buffer (Bio-Rad Laboratories Inc., Hercules, CA, USA) and loaded on a 10 % polyacrylamide gel. Electrophoresis was performed at 90 V (4 °C). Gels were then stained with Coomassie blue, followed by destaining and visualization using a charge-coupled device (CCD) camera.

Calculating the formal net charge of fibrillar SOD1:

As described in the main text, we first determined the number of SOD1 polypeptide chains in an average-sized fibril; to do so, we approximated the volume (V_{SOD1}) and diameter (d_{SOD1}) that a single SOD1 polypeptide would occupy in the fibril according to previously proposed spherical approximation (5) (M represents the molecular weight of the protein):

$$\begin{aligned} V &= (1.212 \times 10^{-3}) \times M \\ V_{SOD1} &= \left(1.212 \times 10^{-3}\right) \times \left(15845\ \text{Da}\right) = 19.2\ \text{nm}^3 \\ d_{SOD1} &= 2 \times \left(\frac{3\times(19.2)}{4\pi}\right)^{1/3} = 3.32\ \text{nm} \end{aligned} \qquad (2)$$

We then approximated a representative length of SOD1 fibrils (L_f) based on TEM images for all three proteins, as well as the average diameter of fibrils (d_f) for each SOD1 protein (d_{avg} in Fig. 5E) in order to calculate the volume of the fibrils (V_f) by assuming a cylindrical geometry for the fibrils:

$$V_f = \pi \left(\frac{d_f}{2}\right)^2 \times L_f \qquad (3)$$

Thus, the number of monomeric SOD1 proteins embedded in a fibril with the volume of V_f can be calculated as:

$$N_{SOD1} = \frac{V_f}{V_{SOD1}} = \frac{V_f}{19.2} \qquad (4)$$

Because there are 11 lysine residues per SOD1 monomer (excluding the acetylation of other residues e.g., serine or threonine), the total number of lysines per fibril can be estimated as:

$$N_{Lys} = 11 \times \frac{V_f}{19.2} = (0.6)V_f \qquad (5)$$

We can then estimate the magnitude of increase in the net negative charge upon "supercharging" of the fibrils directly from the number of lysine residues (since all the lysines become acetylated upon peracetylation, Fig. 6A-C):

$$\Delta Z_f = (0.9)N_{Lys} = (0.9) \times \left(11 \times \frac{V_f}{19.2}\right) = (0.52)V_f \qquad (6)$$

In Equation (6), the constant 0.9 represents the fact that each lysine acetylation increases the net charge of the SOD1 polypeptide by 0.9 units (as described in the main text).

SUPPORTING RESULTS AND DISCUSSION

Acetylation of lysine in SOD1 by aspirin is semi-random.

We expected that the acetylation of the lysine residues in apo-SOD1 with aspirin would be random, with the possible exception of Lys-3 and Lys-91. Nine out of the eleven lysine residues in WT and D90A apo-SOD1 were found to be acetylated (according to MS/MS) regardless of the amount of aspirin added to the solutions, that is, each peak or "rung" in the capillary electropherograms and mass spectra in Fig. 2 were comprised of multiple regioisomers. Approximately 95 % of the apo-SOD1 sequence was observed in the resulting MS/MS spectra, and the statistical scores (X_{COR}, Sequest 1.2) used to grade each MS/MS spectrum were uniformly > 3.0. Lysine-3 was not measured to be acetylated in any WT sample, and Lys-91 was only found to be acetylated in WT apo-SOD1 after addition of the maximum amount of aspirin (Table S1). Because Lys-91 is exposed to solvent, we suspect that it is protected from acetylation because it is located (upon the folding of SOD1) in the most negatively charged region of native SOD1, which will likely raise the pK_a of Lys-ε-NH_3^+ and disfavor acetylation (6). Lysine-91 has been previously shown to be protected from acetylation by acetic anhydride (2). Lysine-3 is located at the dimer interface and might be sterically shielded from reaction.

In the case of A4V apo-SOD1, all lysine residues were found to be acetylated (even Lys-3 and Lys-91) regardless of the concentration of aspirin (Table S1). The ability of aspirin to acetylate Lys-3 and Lys-91 in A4V apo-SOD1 might be facilitated by the conformational instability and high degree of disorder associated with this ALS-variant (7, 8).

SUPPORTING FIGURES

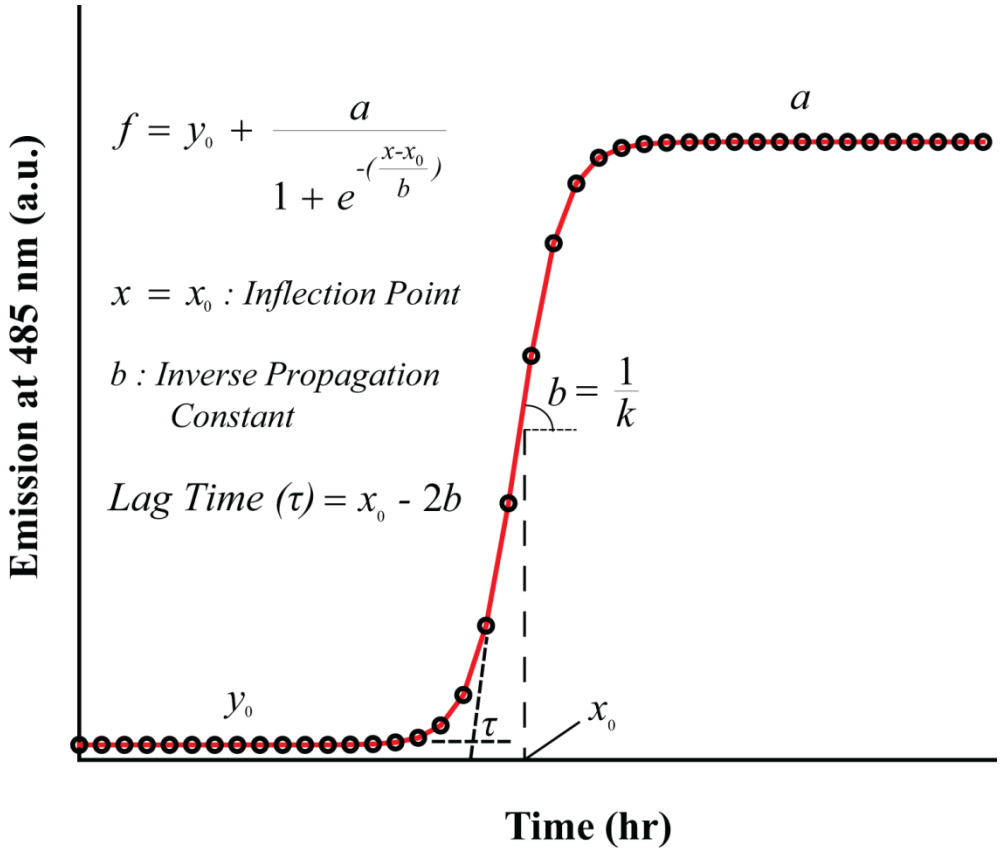

FIGURE S1 Sigmoidal curve used to fit fibrillization kinetics of apo-SOD1 protein variants as measured by an increase in thioflavin-T (ThT) fluorescence at 485 nm.

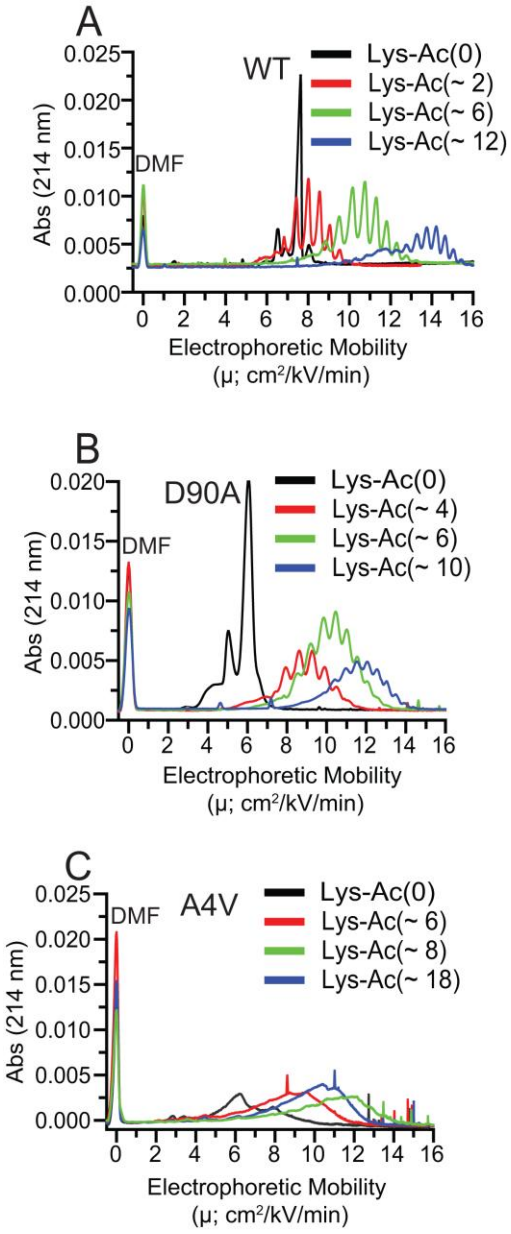

FIGURE S2 Aspirin acetylates lysine residues in WT and ALS-variant apo-SOD1. Capillary electropherograms of soluble (A) WT, (B) D90A, and (C) A4V apo-SOD1 after reaction with different concentrations of aspirin (in aqueous buffer). The mean numbers of acetylated lysines are denoted as "Lys-Ac(~N)", and are listed per apo-SOD1 dimer. DMF (dimethylformamide) was added as a neutral marker of electroosmotic flow.

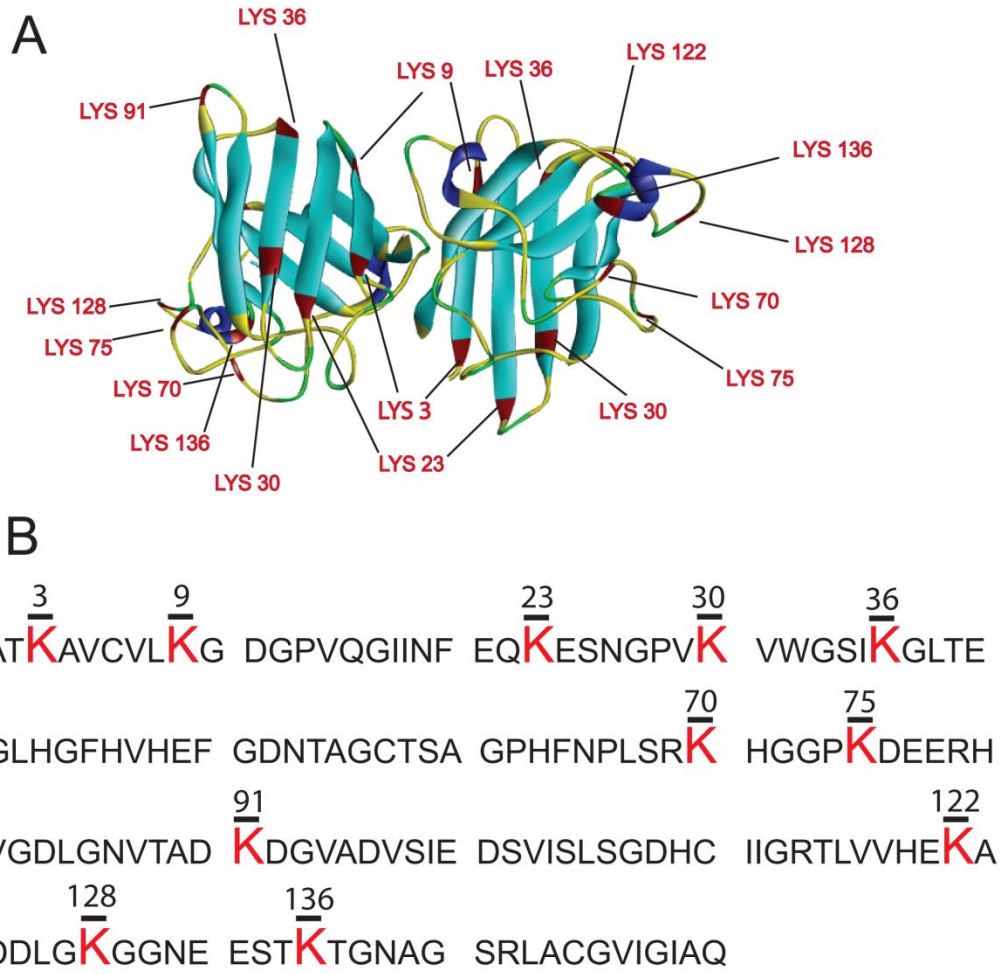

FIGURE S3 Three dimensional structure and amino acid sequence of human SOD1. *(A)* Three dimensional ribbon structure of WT human SOD1 dimer (PDB entry: 2V0A). *(B)* Amino acid sequence of WT human SOD1 (Uniprot entry: SODC_Human). Lysine residues are numbered and colored in red.

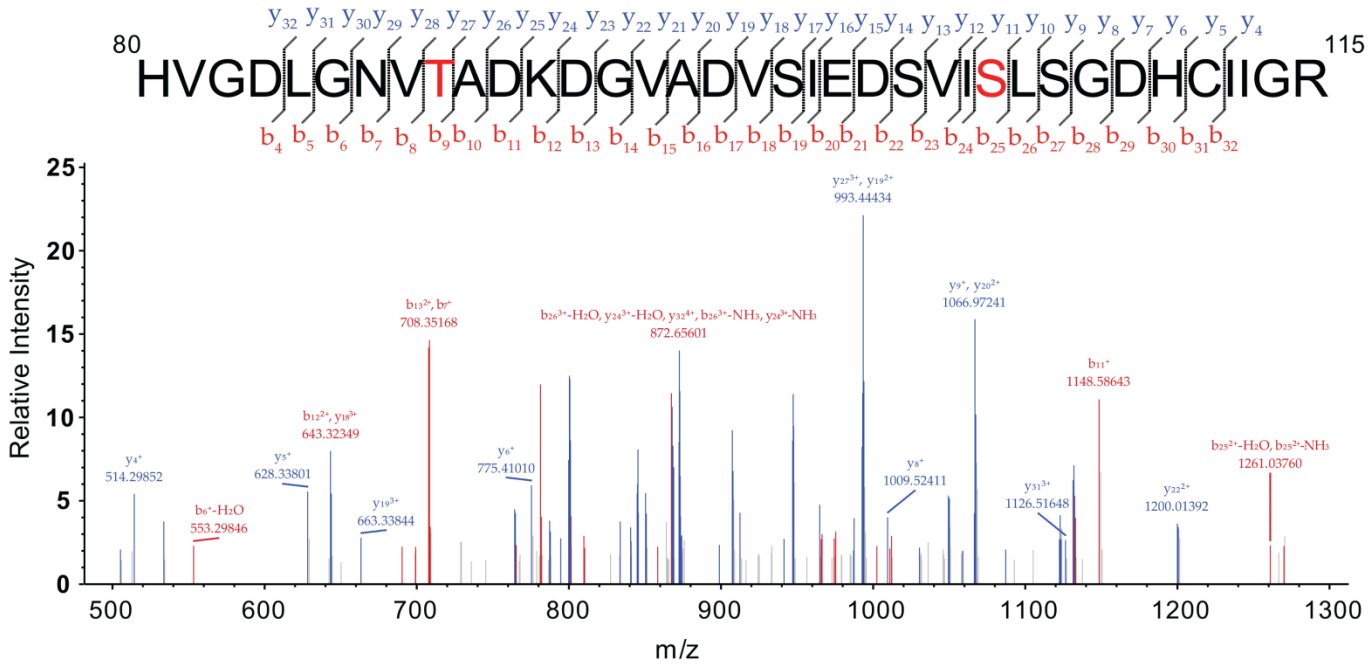

FIGURE S4 High concentration of aspirin can acetylate serine and threonine residues in A4V apo-SOD1. MS/MS spectrum of acetylated peptide 80-115, showing the acetylation of Thr-88 and Ser-105. This peptide was derived from trypsinization of A4V apo-SOD1 that was reacted with 150 mM acetylsalicylic acid (before fibrillization).

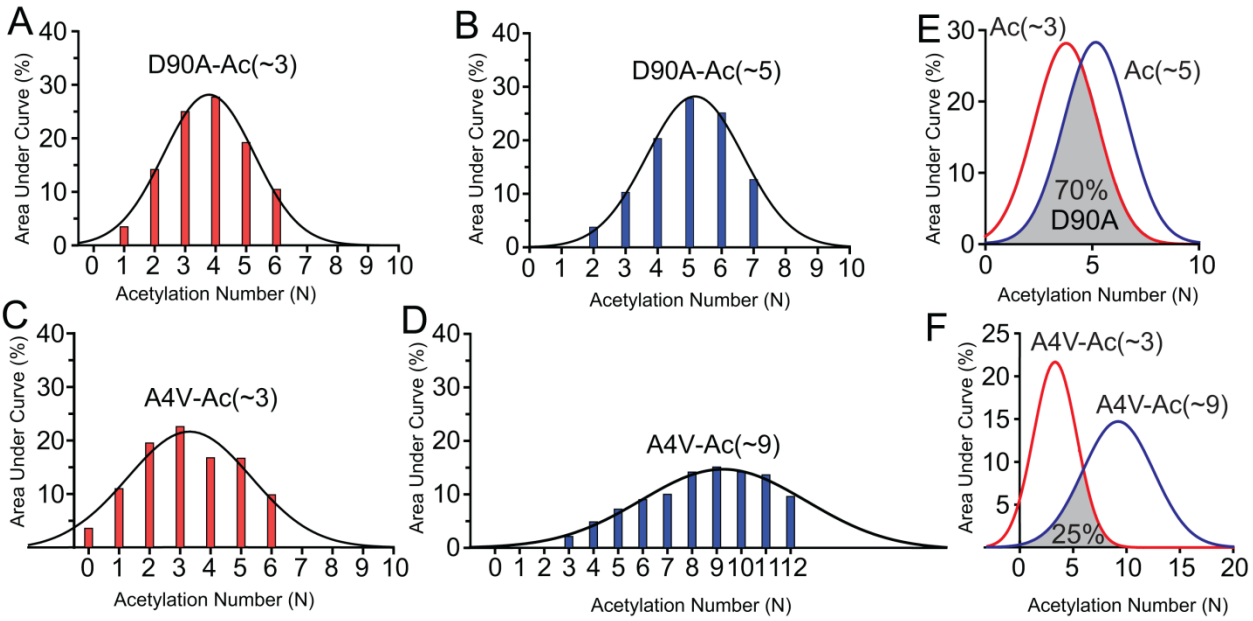

FIGURE S5 Relative concentration of each acetyl derivative in solutions of D90A and A4V apo-SOD1 that were acetylated with aspirin before fibrillization. Percentages were calculated from integration of the mass spectra of *(A-B)* D90A and *(C-D)* A4V apo-SOD1 (these spectra are shown in Fig. 2 of main text). Gaussian distribution for each mass envelope is plotted with $R^2 > 0.99$. The degree by which MS Gaussian distributions overlap for each acetylation number (median) is illustrated for *(E)* D90A and *(F)* A4V apo-SOD1.

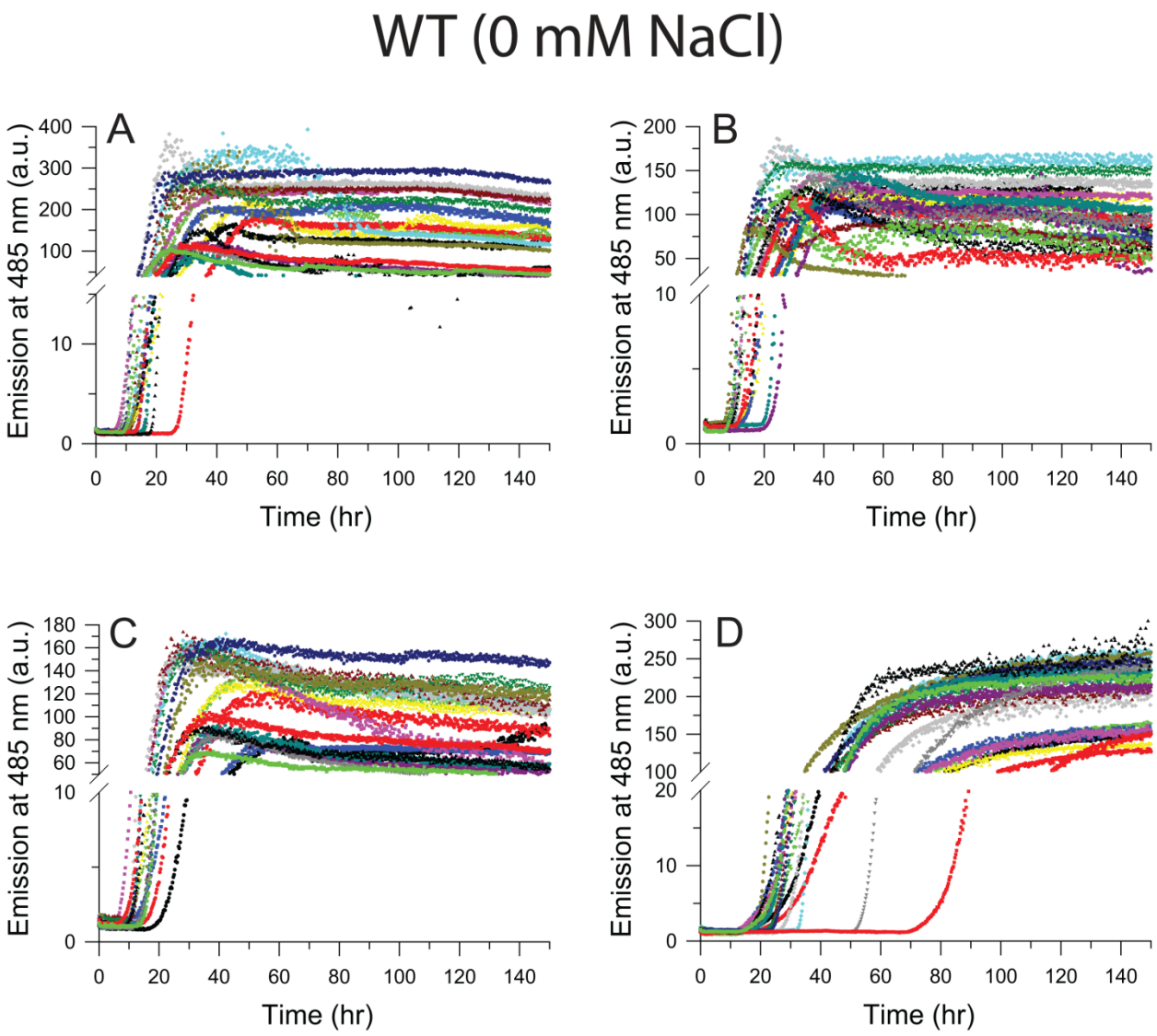

FIGURE S6 Fibrillization of unacetylated and acetylated WT apo-SOD1 as measured by thioflavin-T fluorescence in a 96-well microplate in 0 mM NaCl. *(A-D)* Raw, unnormalized thioflavin-T fluorescence amyloid assays for all 18 replicates of unacetylated and acetylated WT apo-SOD1 at pH 7.4 in 0 mM NaCl. *(A)* Lys-Ac(0), *(B)* Lys-Ac(~1), *(C)* Lys-Ac(~3), and *(D)* Lys-Ac(~6). The number of acetylated lysine residues is listed per apo-SOD1 monomer.

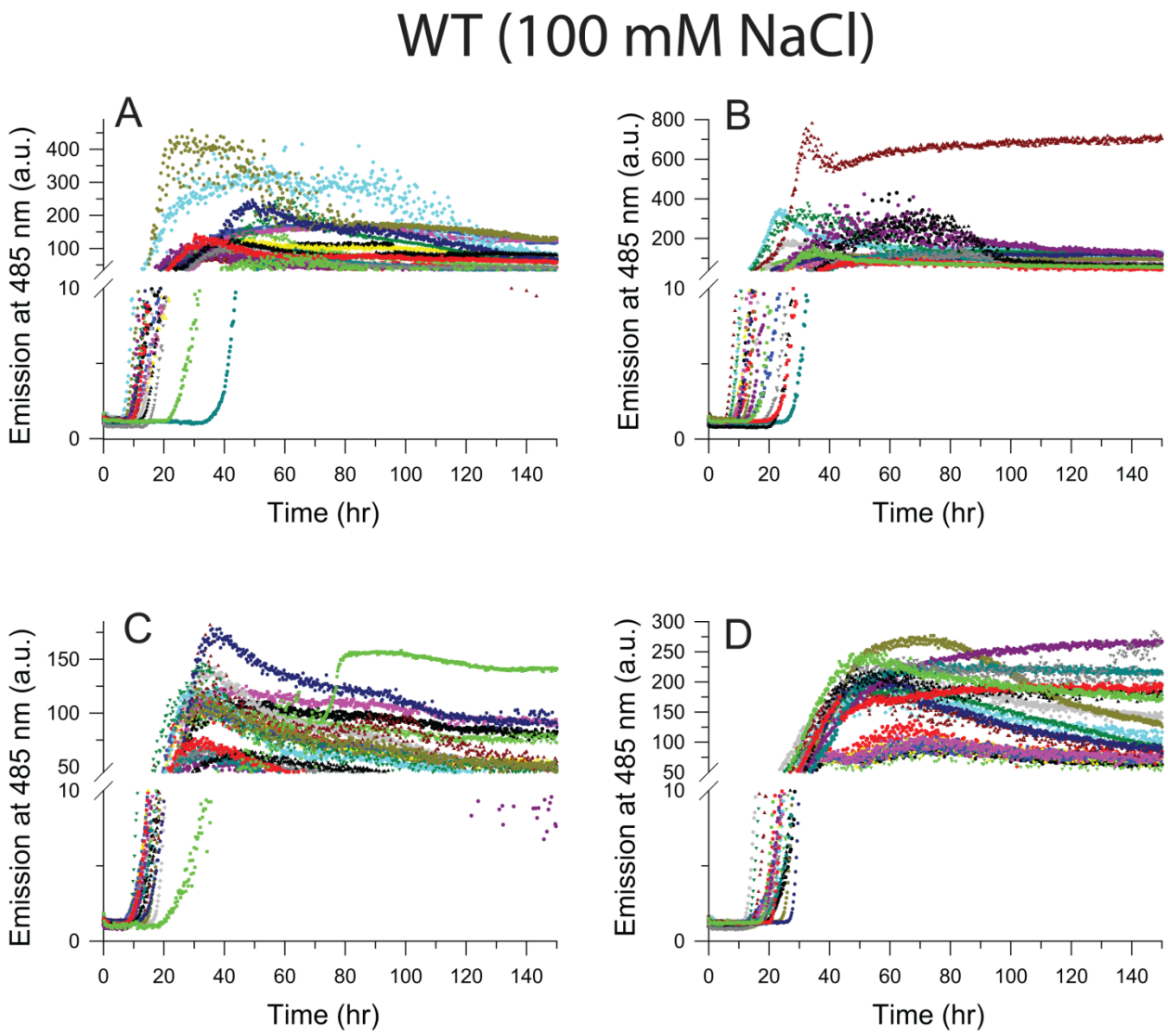

FIGURE S7 Fibrillization of unacetylated and acetylated WT apo-SOD1 as measured by thioflavin-T fluorescence in a 96-well microplate in 100 mM NaCl. *(A-D)* Raw, unnormalized thioflavin-T fluorescence amyloid assays for all 18 replicates of unacetylated and acetylated WT apo-SOD1 at pH 7.4 in 100 mM NaCl. *(A)* Lys-Ac(0), *(B)* Lys-Ac(~1), *(C)* Lys-Ac(~3), and *(D)* Lys-Ac(~6). The number of acetylated lysine residues is listed per apo-SOD1 monomer.

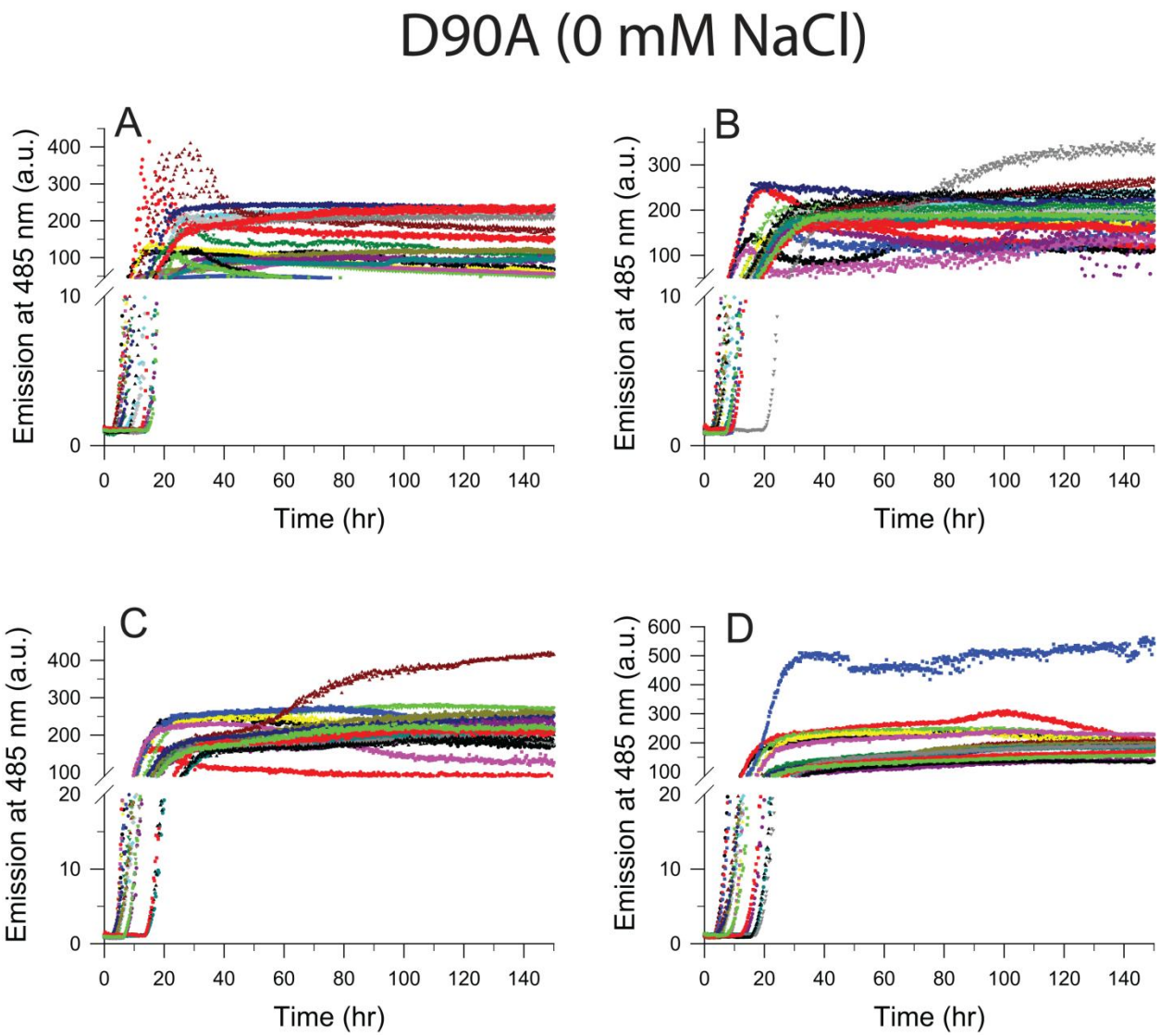

FIGURE S8 Fibrillization of unacetylated and acetylated D90A apo-SOD1 as measured by thioflavin-T fluorescence in a 96-well microplate in 0 mM NaCl. *(A-D)* Raw, unnormalized thioflavin-T fluorescence amyloid assays for all 18 replicates of unacetylated and acetylated D90A apo-SOD1 at pH 7.4 in 0 mM NaCl. *(A)* Lys-Ac(0), *(B)* Lys-Ac(~2), *(C)* Lys-Ac(~3), and *(D)* Lys-Ac(~5). The number of acetylated lysine residues is listed per apo-SOD1 monomer.

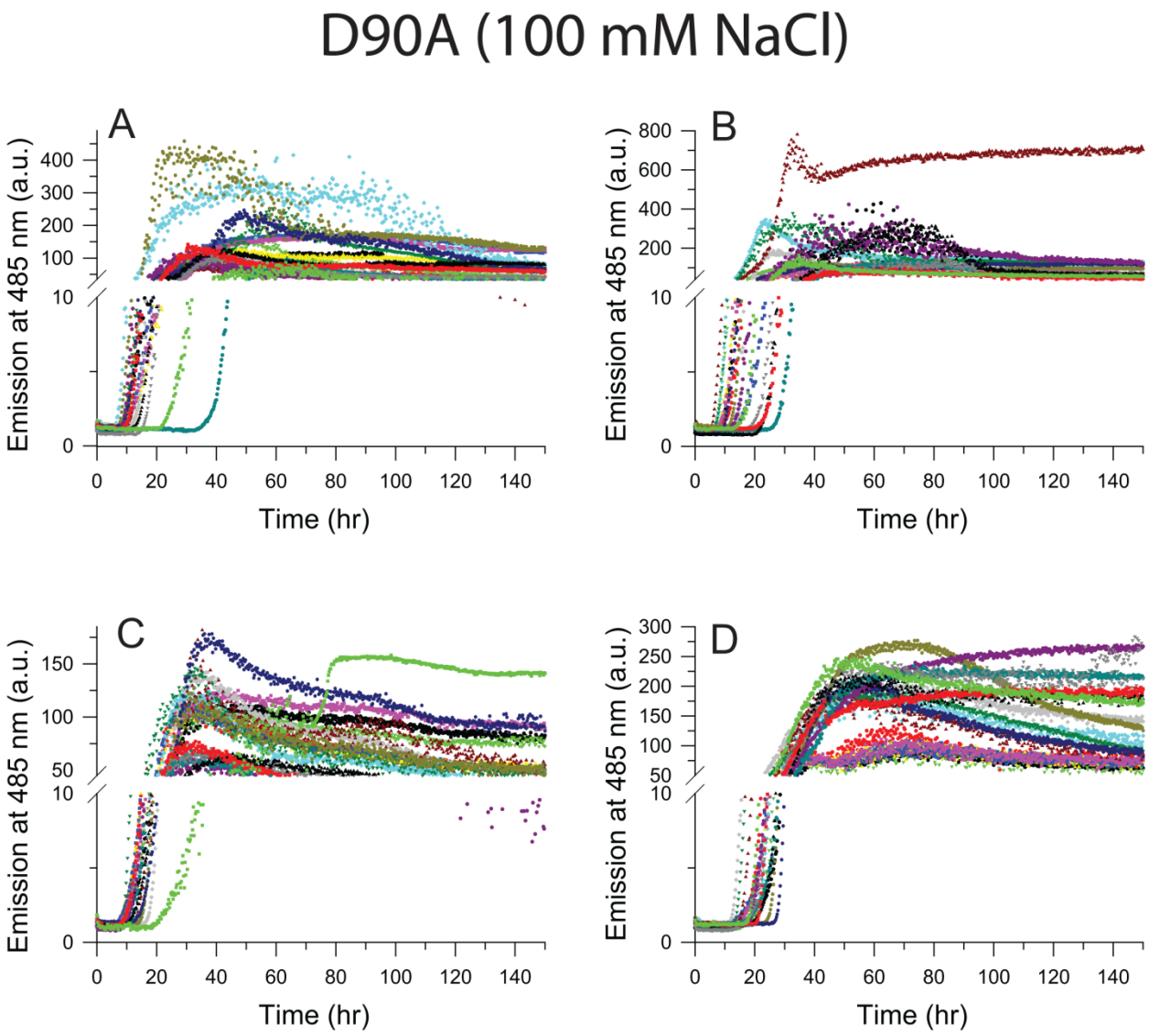

FIGURE S9 Fibrillization of unacetylated and acetylated D90A apo-SOD1 as measured by thioflavin-T fluorescence in a 96-well microplate in 100 mM NaCl. *(A-D)* Raw, unnormalized thioflavin-T fluorescence amyloid assays for all 18 replicates of unacetylated and acetylated D90A apo-SOD1 at pH 7.4 in 100 mM NaCl. *(A)* Lys-Ac(0), *(B)* Lys-Ac(~2), *(C)* Lys-Ac(~3), and *(D)* Lys-Ac(~5). The number of acetylated lysine residues is listed per apo-SOD1 monomer.

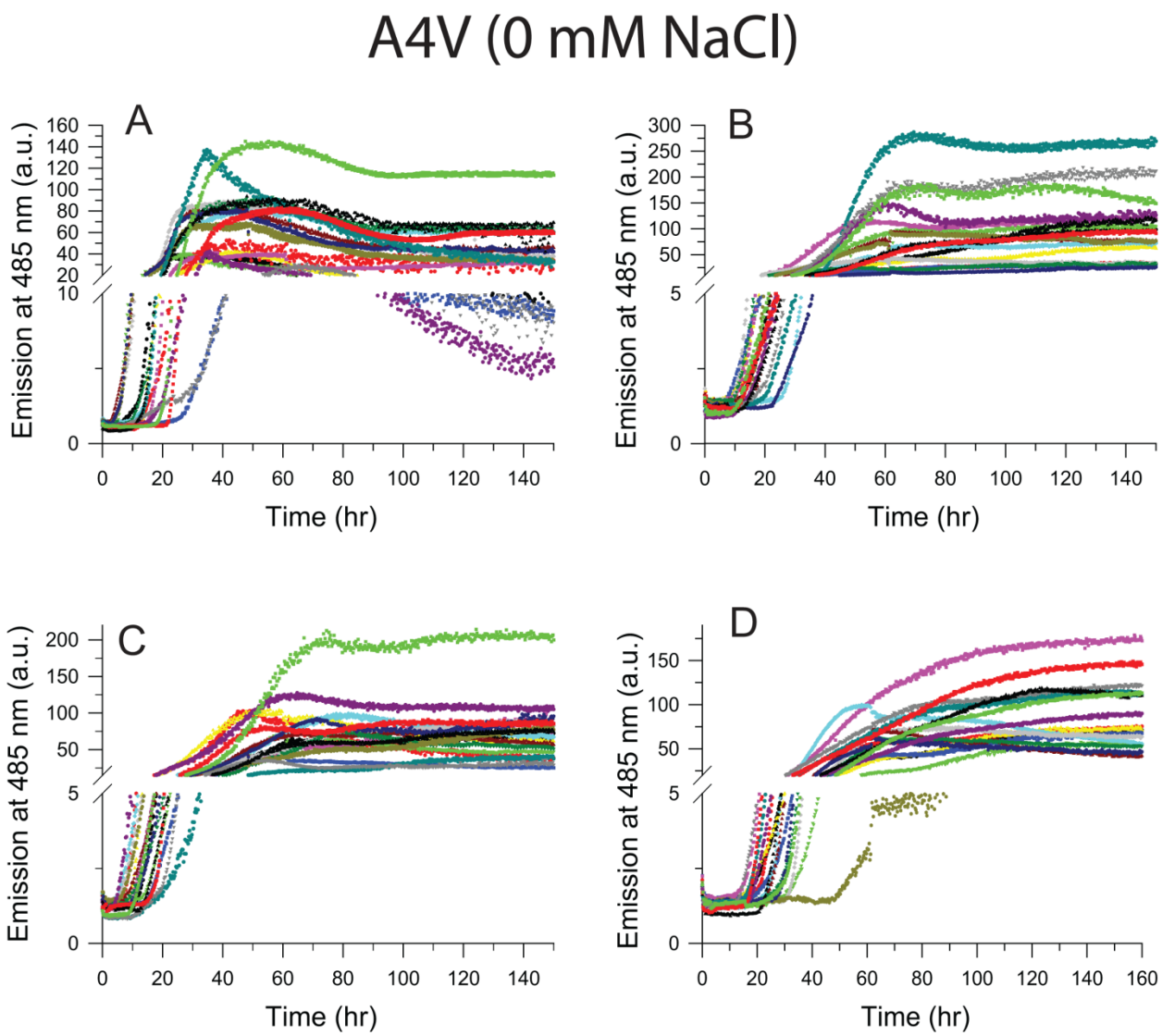

FIGURE S10 Fibrillization of unacetylated and acetylated A4V apo-SOD1 as measured by thioflavin-T fluorescence in a 96-well microplate in 0 mM NaCl. *(A-D)* Raw, unnormalized thioflavin-T fluorescence amyloid assays for all 18 replicates of unacetylated and acetylated A4V apo-SOD1 at pH 7.4 in 0 mM NaCl. *(A)* Lys-Ac(0), *(B)* Lys-Ac(~3), *(C)* Lys-Ac(~4), and *(D)* Lys-Ac(~9). The number of acetylated lysine residues is listed per apo-SOD1 monomer.

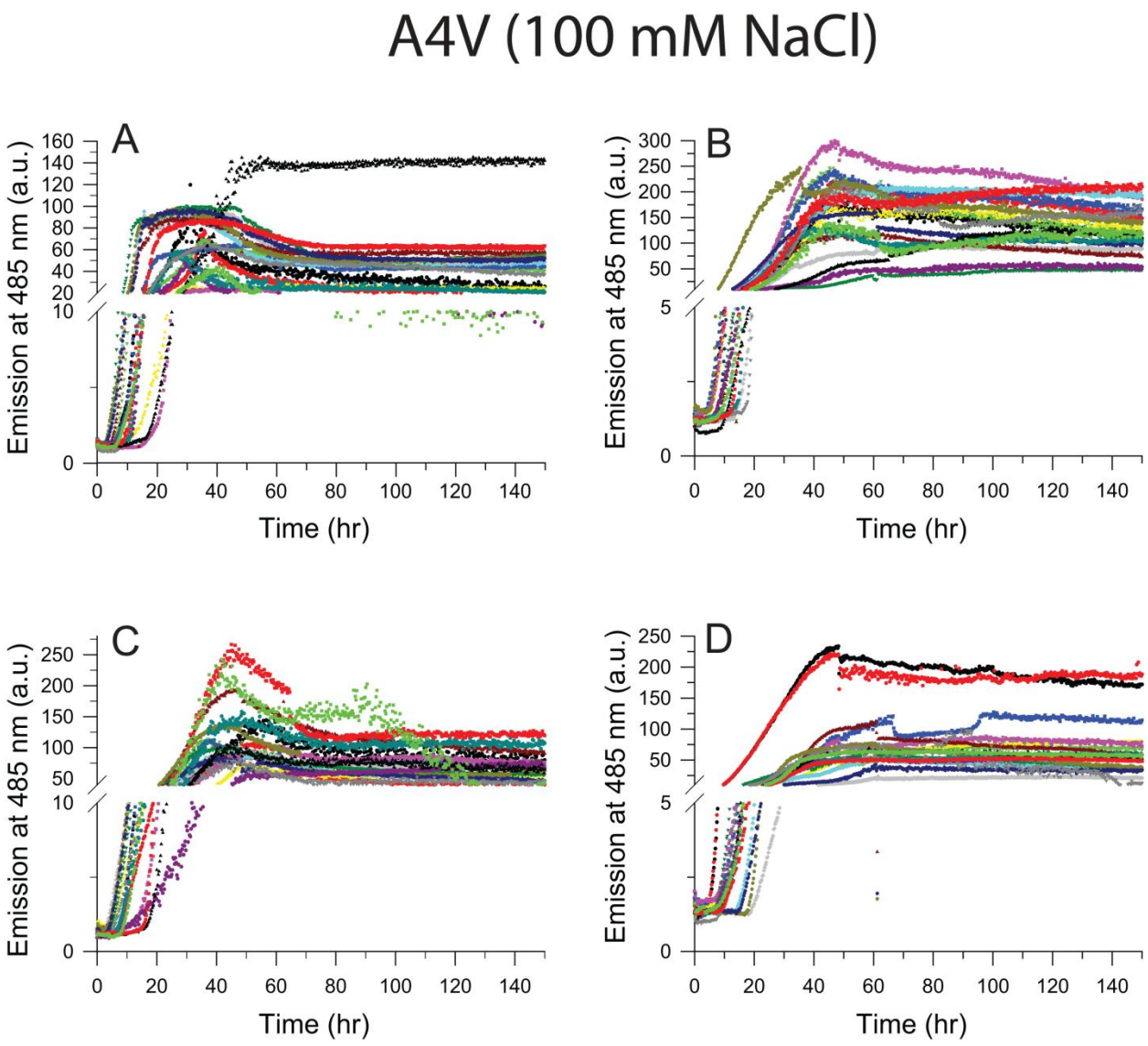

FIGURE S11 Fibrillization of unacetylated and acetylated A4V apo-SOD1 as measured by thioflavin-T fluorescence in a 96-well microplate in 100 mM NaCl. *(A-D)* Raw, unnormalized thioflavin-T fluorescence amyloid assays for all 18 replicates of unacetylated and acetylated A4V apo-SOD1 at pH 7.4 in 100 mM NaCl. *(A)* Lys-Ac(0), *(B)* Lys-Ac(~3), *(C)* Lys-Ac(~4), and *(D)* Lys-Ac(~9). The number of acetylated lysine residues is listed per apo-SOD1 monomer.

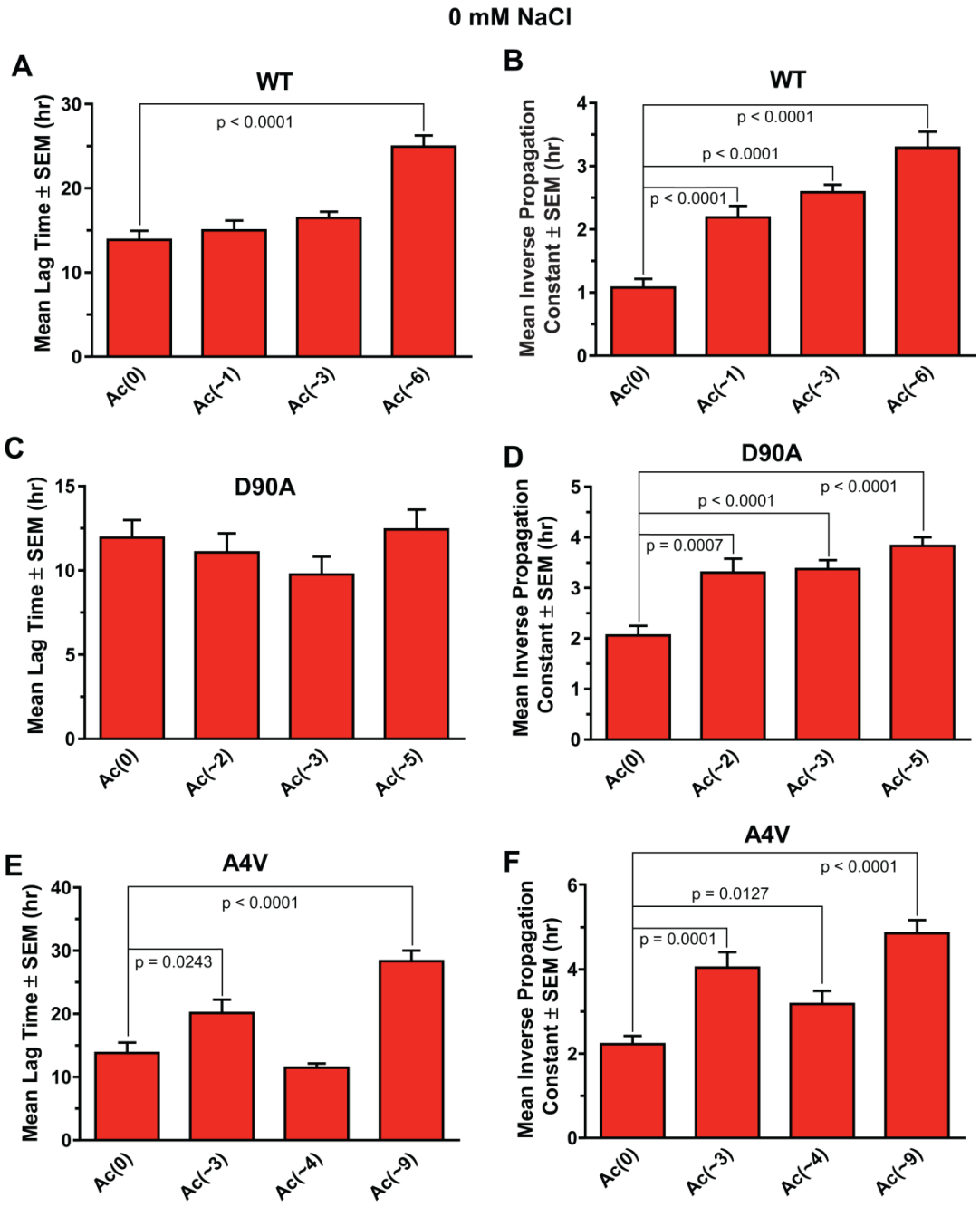

FIGURE S12 Statistical comparison of mean lag time and mean inverse propagation constant (from Table 1 in main text) for fibrillization of unacetylated and acetylated apo-SOD1 proteins in 0 mM NaCl. *(A-B)* WT, *(C-D)* D90A, and *(E-F)* A4V apo-SOD1 at different degrees of acetylation (in 0 mM NaCl). P-values compare the acetylated derivative with the unacetylated protein, and were calculated with a Student's unpaired t-test at a 95 % confidence interval. The number of acetylated lysine residues is listed per apo-SOD1 monomer. A lack of statistical significance ($p > 0.05$) between the unacetylated form of each protein, and anyone of its acetylated derivatives is indicated by the absence of a listed p-value and the absence of a connecting line. Data represent the calculated mean ± SEM for 18 replicates ($n = 18$).

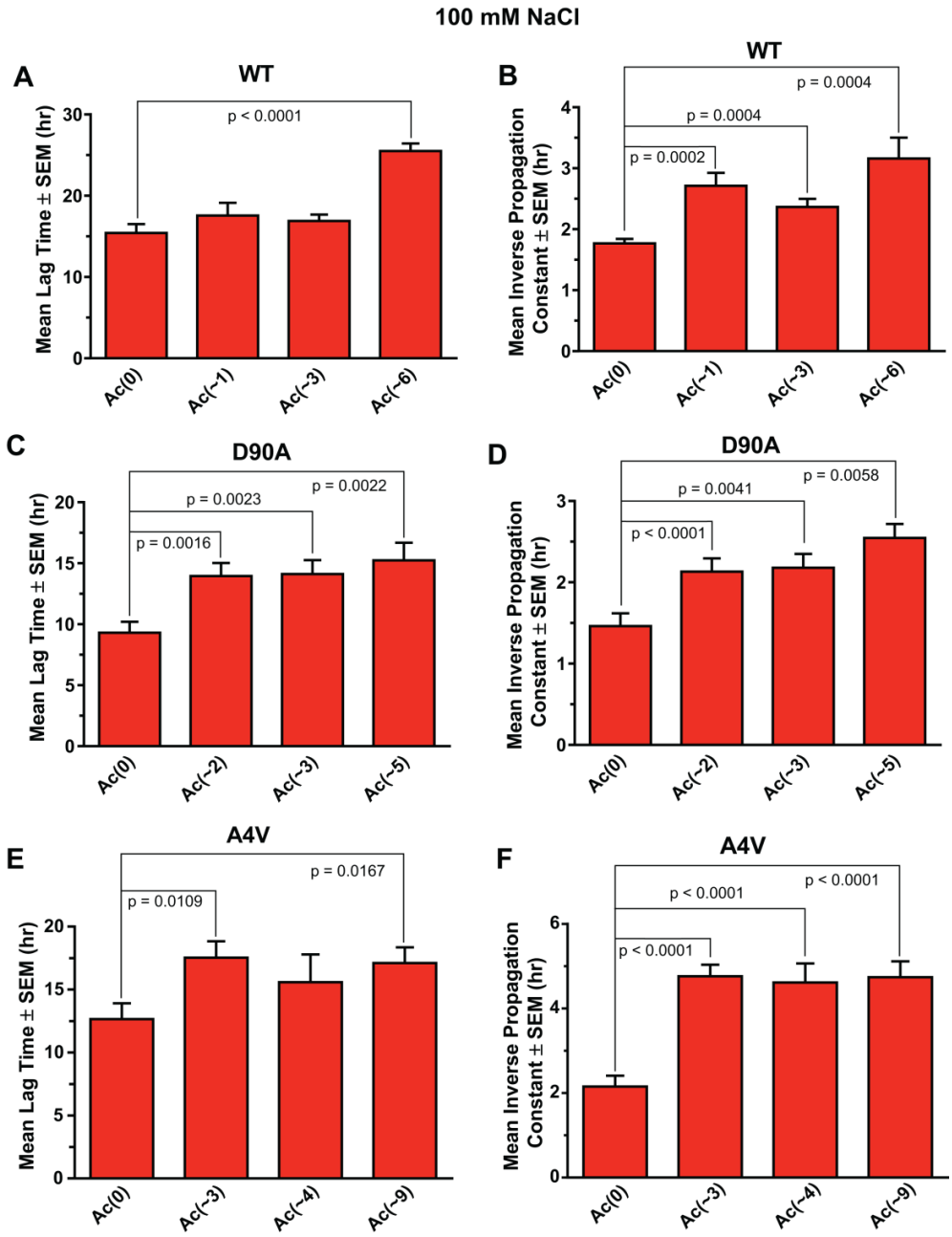

FIGURE S13 Statistical comparison of mean lag time and mean inverse propagation constant (from Table 1 in main text) for fibrillization of unacetylated and acetylated apo-SOD1 proteins in 100 mM NaCl. *(A-B)* WT, *(C-D)* D90A, and *(E-F)* A4V apo-SOD1 at different degrees of acetylation (in 100 mM NaCl). P-values compare the acetylated derivative with the unacetylated protein, and were calculated with a Student's unpaired t-test at a 95 % confidence interval. The number of acetylated lysine residues is listed per apo-SOD1 monomer. A lack of statistical significance ($p > 0.05$) between the unacetylated form of each protein, and anyone of its acetylated derivatives is indicated by the absence of a listed p-value and the absence of a connecting line. Data represent the calculated mean ± SEM for 18 replicates ($n = 18$).

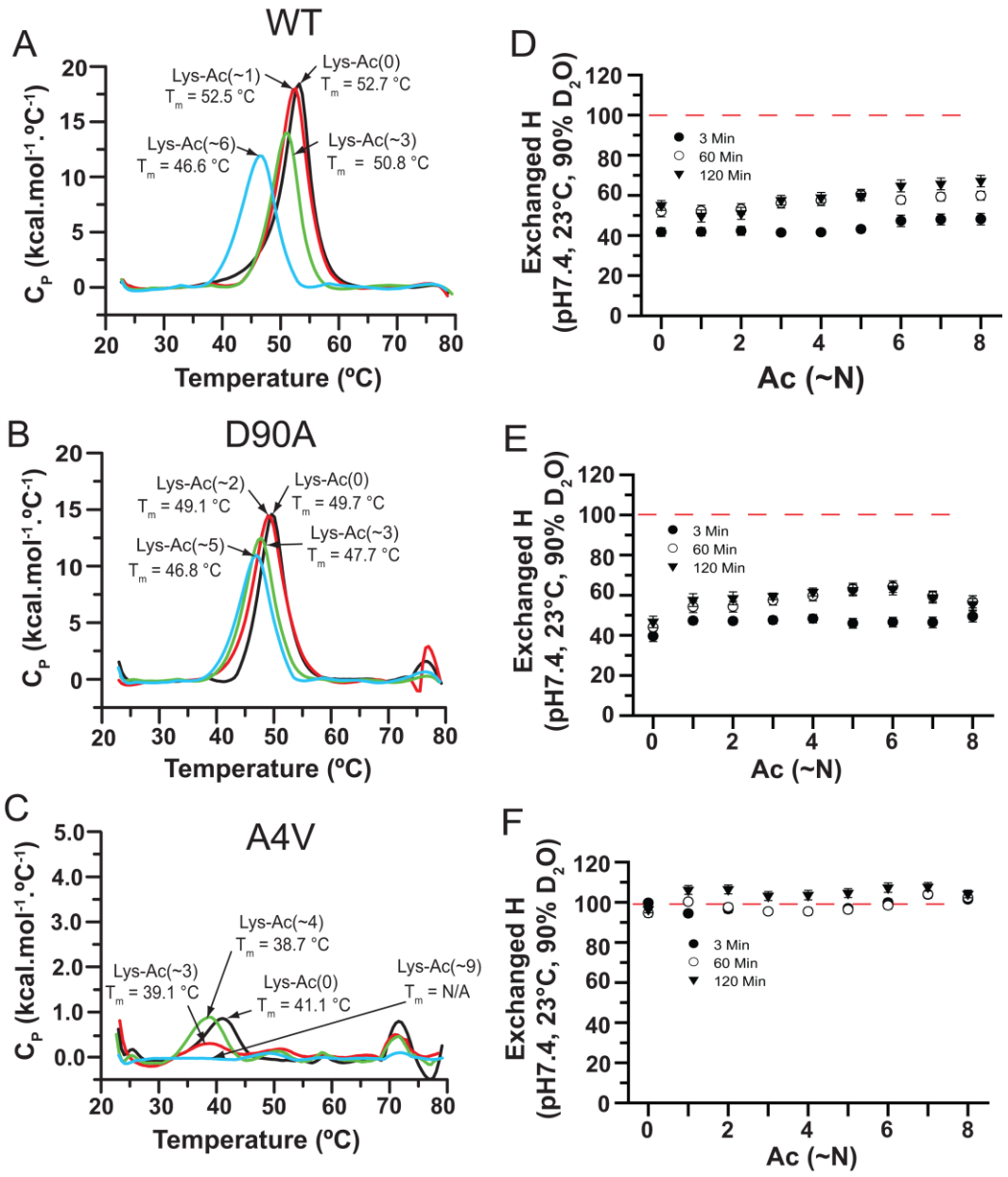

FIGURE S14 Differential scanning calorimetry and H/D exchange of unacetylated and acetylated apo-SOD1 proteins. *(A-C)* Thermograms of WT, D90A, and A4V apo-SOD1 are shown as a function of acetylated lysines. *(D-F)* Plots of number of exchanged hydrogens versus acetylation number for WT, D90A, and A4V apo-SOD1. Samples were incubated in 90 % D_2O at three different time points. Red dashed line indicates the experimental limit of deuteration (i.e., the number of exchanged hydrogen in the thermally denatured and perdeuterated protein). The extent of back-exchange for each acetylated derivative of each protein was measured. Typical values of back-exchange were 38 % (WT), 29 % (D90A), and 24 % (A4V) and the rate of back-exchange was not affected by the extent of acetylation. Mean number of acetylated lysine residues is denoted as Lys-Ac(~N) in each panel. In panel *(C)*, the endothermic transitions of unmodified and minimally acetylated A4V were low in intensity to begin with, which

suggested that the A4V apo-SOD1 protein was populating folded and unfolded states (as previously reported for this unstable ALS-variant (9)). A similar conclusion about low stability of A4V apo-SOD1 protein can be deduced from plots of HDX in panel *(F)*. The number of acetylated lysine residues is listed per apo-SOD1 monomer.

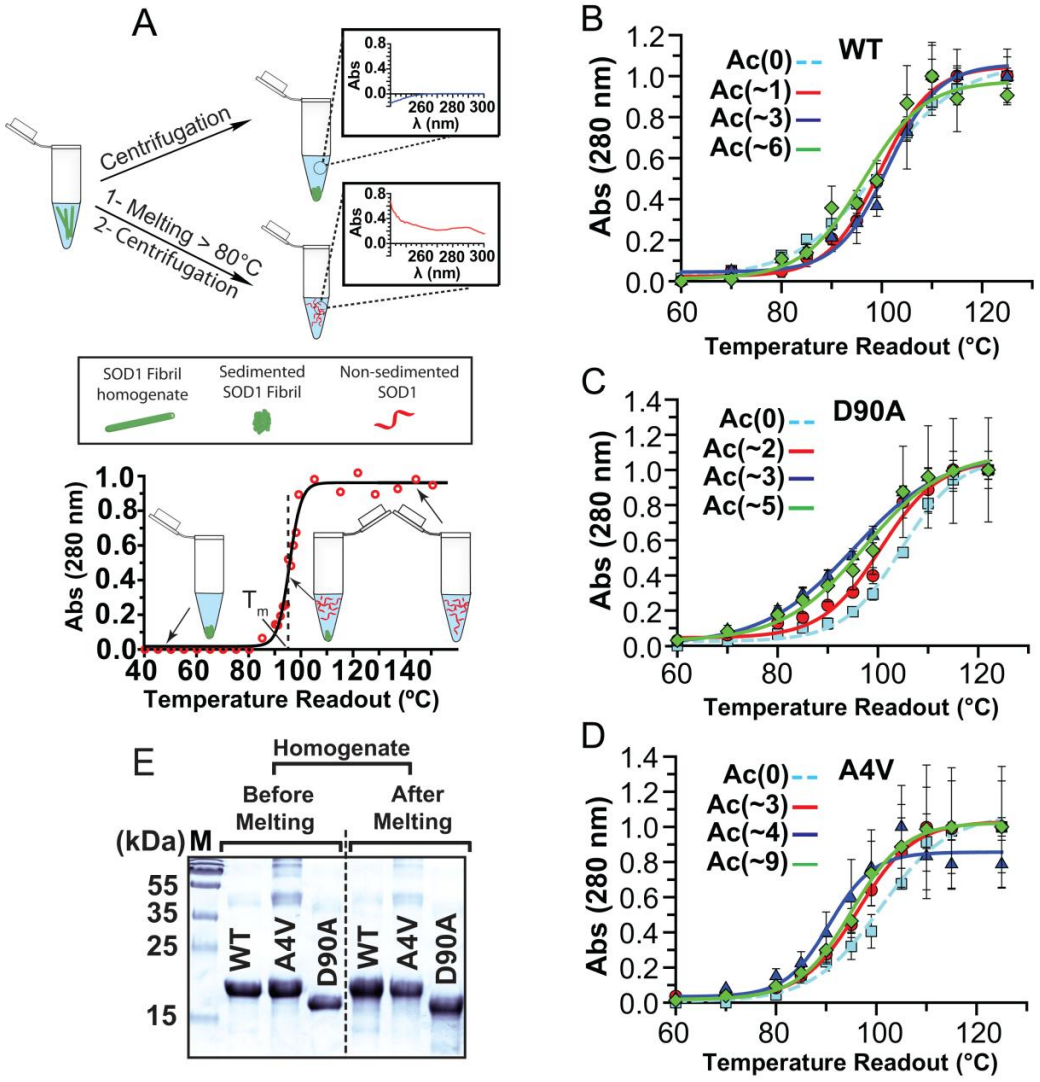

FIGURE S15 Effect of lysine acetylation in native apo-SOD1 on thermostability of resulting amyloid fibrils (i.e., acetylation before fibrillization). *(A)* Schematic illustration of thermal defibrillization assay for determining melting temperature of fibrillar apo-SOD1. Solutions of fibrillar SOD1 are heated, centrifuged, and the supernatant is analyzed with UV-Vis spectrophotometry. Soluble SOD1 proteins are retained in supernatant upon thermal defibrillization. T_m values (lower panel) were calculated as the inflection point of the sigmoid (x_0 in Equation (1) of Supporting Information). *(B-D)* Thermal defibrillization curves of fibrils formed from unacetylated and acetylated *(B)* WT, *(C)* D90A, and *(D)* A4V native apo-SOD1 proteins. Number of acetylated lysines is listed per apo-SOD1 monomer. Data are presented as mean ± SEM (n = 4), and all fittings resulted in R^2 = 0.99. *(E)* Reducing SDS-PAGE on

unacetylated apo-SOD1 amyloid fibrils before melting (left) and after the completion of melting (right). Intermediate increases in the mean number of acetylated lysines did not consistently result in statistically significant differences in fibril T_m. We suspect that these similarities in fibril T_m occurred because these mixtures have overlapping degrees of acetylation in spite of different mean number of acetylation. For example, the T_m of D90A-Ac(~3) apo-SOD1 fibrils is statistically similar to the T_m of D90A-Ac(~5) fibrils ($p > 0.05$, Fig. S15C and Table S5). The T_m values for A4V-Ac(~3) and A4V-Ac(~9) are statistically similar ($p > 0.05$, Fig. S15D and Table S5). Accordingly, we found ~ 70 % overlap between the distribution of acetyl groups of D90A apo-SOD1-Ac(~3) and D90A apo-SOD1-Ac(~5) (Fig. S5E) and ~ 25 % overlap between A4V apo-SOD1-Ac(~3) and A4V apo-SOD1-Ac(~9) (Fig. S5F). This overlap might explain the statistically similar average T_m values between these different mixtures (Fig. S15B-D).

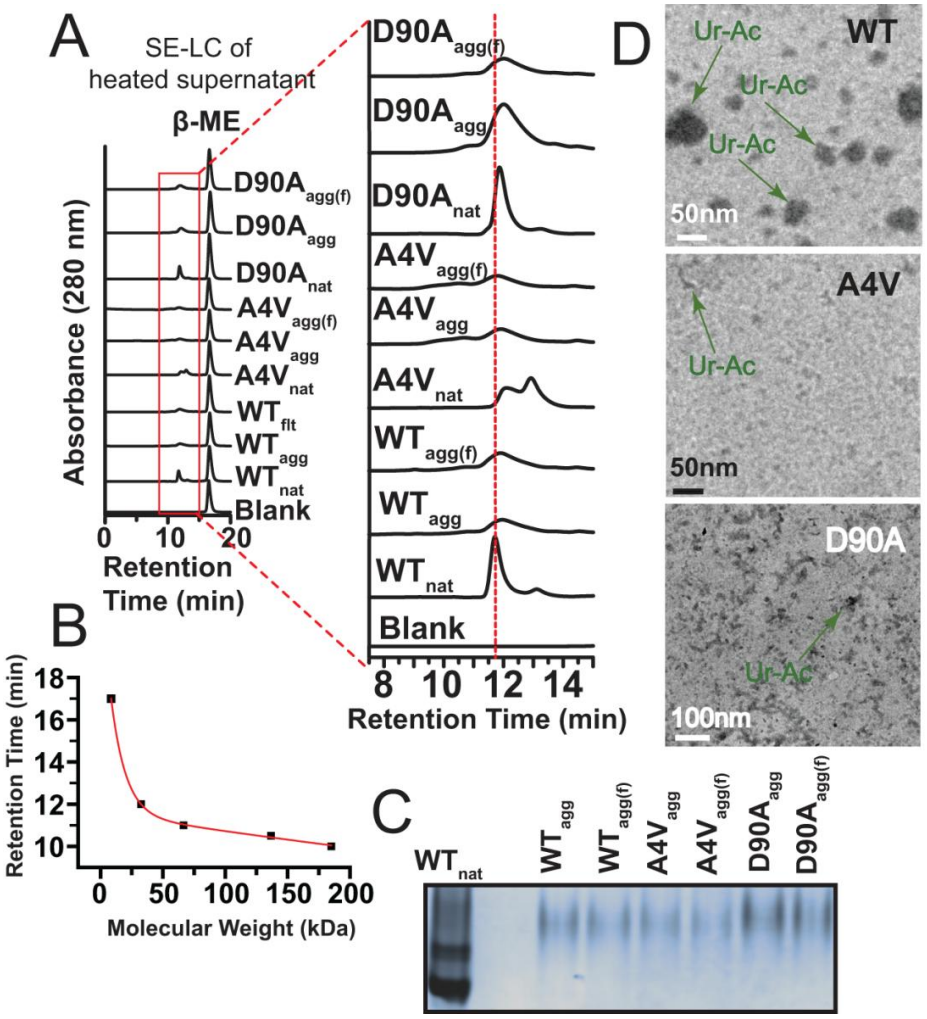

FIGURE S16 Characterization of state of oligomerization of WT and ALS-linked apo-SOD1 after thermal defibrillization of amyloid fibrils of apo-SOD1. *(A)* Size-exclusion chromatograms of supernatants of heated fibrils with native state (dimer) of each protein as control; β-ME stands for β-mercaptoethanol. Supernatants of samples heated at 125 °C (defibrillized proteins) were combined with β-mercaptoethanol (60:1 v/v ratio) to prevent disulfide cross-linking between cysteine residues during cooling period. *(B)* Calibration curve used for size determination of thermally defibrillized species in supernatants. *(C)* Native PAGE (10 %) performed on supernatant of melted fibrils with WT apo-SOD1 (dimer) as control. *(D)* TEM images of melted fibrils from supernatant. Ur-Ac indicates the clusters of uranyl acetate dye. Scale bars in *(D)* are 50 nm in case of WT and A4V and 100 nm in case of D90A. Subscripts "agg" and "agg(f)" in *(A-C)* indicate melted unfiltered protein aggregates and those that were filtered with a 0.2 μm filter, respectively. Subscript "nat" in *(A)* and *(C)* designates the native protein.

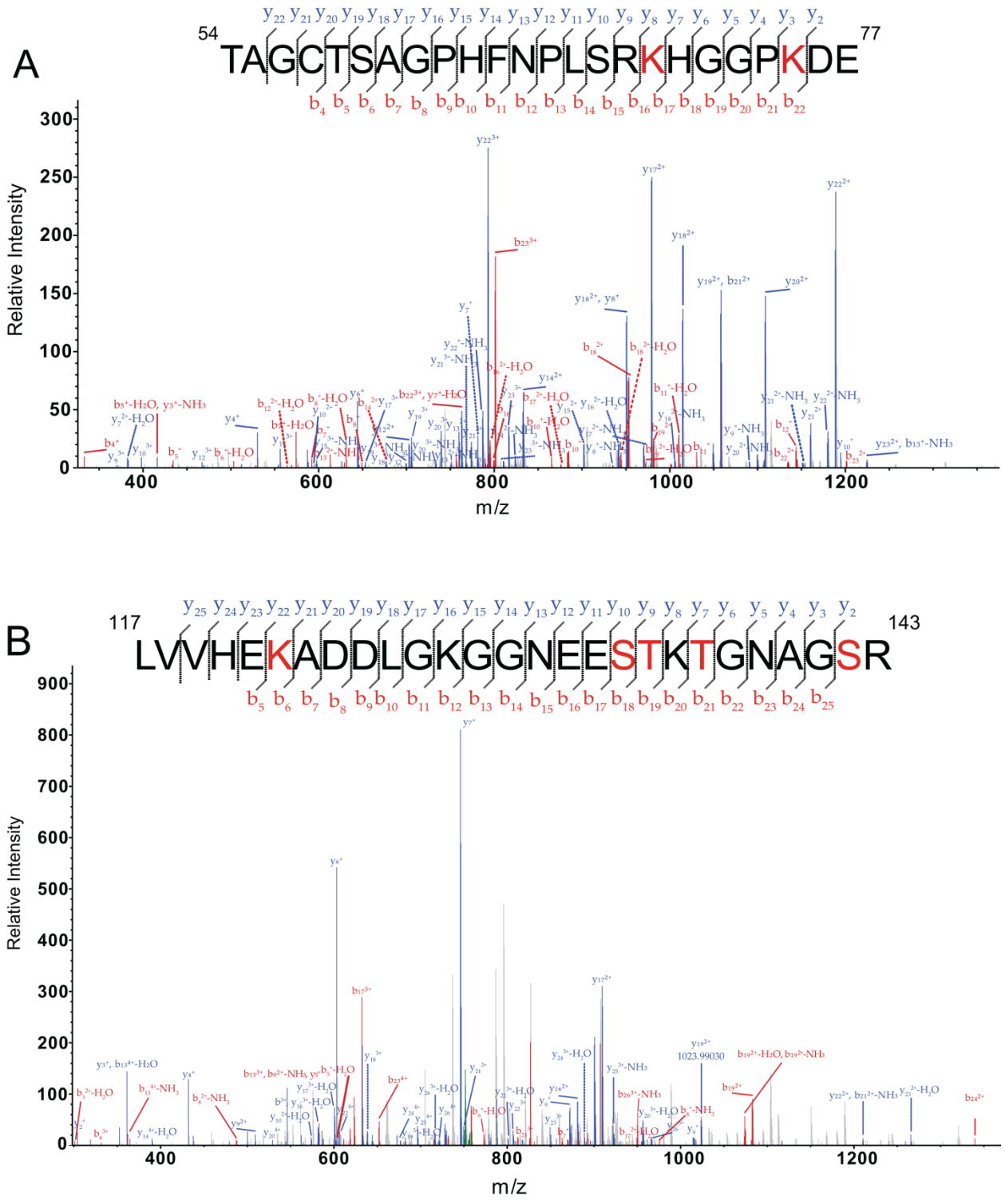

FIGURE S17 MS/MS spectra of tryptic SOD1 peptides from WT apo-SOD1 fibrils that were acetylated with aspirin after fibrillization. *(A)* MS/MS spectrum of peptide comprised of residues 54-77; *(B)* MS/MS spectrum of residues 117-143.

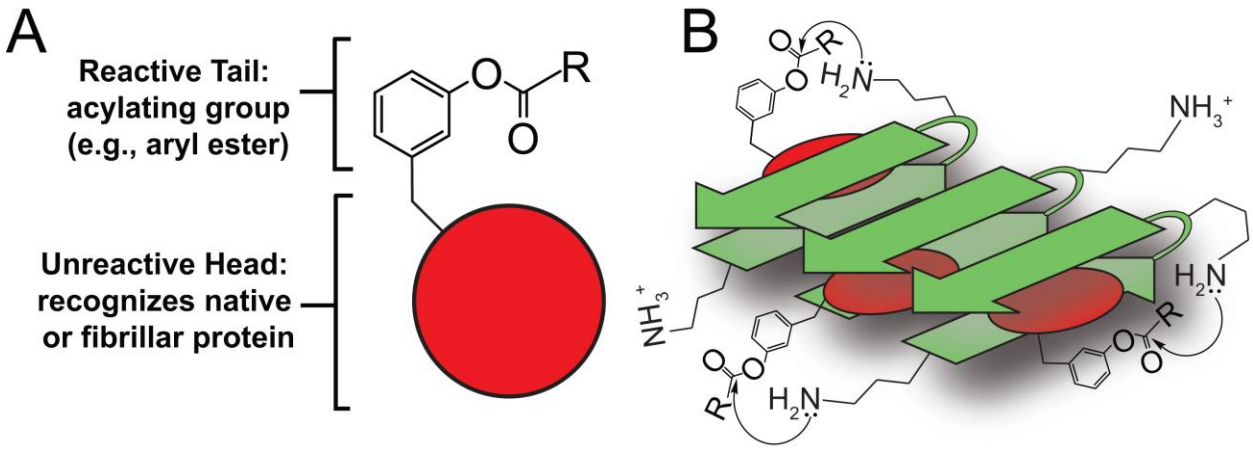

FIGURE S18 *(A)* Chemical anatomy of a prototype "charge boosting" drug that contains a "head" that either binds to a native protein or partitions to an amyloid-like oligomer, and an acylating "tail" that modifies nearby lysine residues. *(B)* The "head" does not become covalently attached to the protein, and can be displaced over time to allow for the binding and reaction of additional "charge boosters". This scheme does not intend to indicate a preferred mode of binding (perpendicular or parallel to β-sheets). Designing acylating agents that specifically bind to and acylate lysine in anionic amyloid-like oligomers is certainly feasible. Several natural and synthetic small-molecules have been shown to bind to amyloid fibrils formed from different proteins (10). We hypothesize that synthetically linking aryl ester moieties to these amyloid-binding molecules might enable the selective (and successive) acylation of amyloid fibrils.

TABLE S1 Results of tandem mass spectrometry of trypsin and pepsin digests of WT and ALS-variant apo-SOD1 at varying degrees of acetylation; (•) represents the acetylated lysine residues in digested fragments. N represents the number of acetylated lysine residues listed per apo-SOD1 monomer.

	Mean Ac(~N)	**Lysine residue number**										
		3	9	23	30	36	70	75	91	122	128	136
WT	0											
	1		•	•	•	•	•	•		•	•	•
	3		•	•	•	•	•	•		•	•	•
	6		•	•	•	•	•	•	•	•	•	•
	Mean Ac(~N)	**Lysine residue number**										
		3	9	23	30	36	70	75	91	122	128	136
D90A	0											
	2		•	•	•	•	•	•		•	•	•
	3		•	•	•	•	•	•		•	•	•
	5		•	•	•	•	•	•		•	•	•
	Mean Ac(~N)	**Lysine residue number**										
		3	9	23	30	36	70	75	91	122	128	136
A4V	0											
	3	•	•	•	•	•	•	•	•	•	•	•
	4	•	•	•	•	•	•	•	•	•	•	•
	9	•	•	•	•	•	•	•	•	•	•	•

TABLE S2 Average kinetic parameters of ThT aggregation assays for acetylated and unacetylated WT SOD1, in 0 mM and 100 mM NaCl. All data are presented as mean ± SEM, n = 18. The number of acetylated lysine residues is listed per apo-SOD1 monomer.

SOD1	a (maximum) (a.u.)	x_0 (hr)	b (hr)	Lag time (hr)	Average R^2
WT-Ac(0)	199.2 ± 18.1	16.0 ± 1.1	1.1 ± 0.1	13.9 ± 1.1	0.99
WT-Ac(~1)	127.3 ± 5.5	19.4 ± 1.4	2.2 ± 0.2	15.0 ± 1.2	0.99
WT-Ac(~3)	116.9 ± 8.0	21.6 ± 0.9	2.6 ± 0.1	16.5 ± 0.7	0.99
WT-Ac(~6)	205.9 ± 11.1	31.5 ± 1.3	3.3 ± 0.3	24.9 ± 1.3	0.99
WT-Ac(0) (100 mM NaCl)	166.7 ± 25.8	18.9 ± 1.1	1.8 ± 0.1	15.4 ± 1.1	0.98
WT-Ac(~1) (100 mM NaCl)	191.4 ± 36.4	23.0 ± 1.7	2.7 ± 0.2	17.6 ± 1.6	0.98
WT-Ac(~3) (100 mM NaCl)	98.6 ± 6.8	21.6 ± 0.8	2.4 ± 0.1	16.9 ± 0.8	0.98
WT-Ac(~6) (100 mM NaCl)	169.6 ± 16.7	31.8 ± 1.1	3.2 ± 0.3	25.5 ± 0.9	0.99

TABLE S3 Average kinetic parameters of ThT aggregation assays for acetylated and unacetylated D90A apo-SOD1, in 0 mM and 100 mM NaCl. All data are presented as mean ± SEM, n = 18. The number of acetylated lysine residues is listed per apo-SOD1 monomer.

SOD1	a (maximum) (a.u.)	x_0 (hr)	b (hr)	Lag time (hr)	Average R^2
D90A-Ac(0)	154.6 ± 20.2	16.1 ± 1.3	2.1 ± 0.2	11.9 ± 1.0	0.98
D90A-Ac(~2)	189.4 ± 8.9	17.7 ± 1.3	3.3 ± 0.3	11.1 ± 1.1	0.99
D90A-Ac(~3)	188.4 ± 11.8	16.5 ± 1.1	3.4 ± 0.2	9.8 ± 1.1	0.99
D90A-Ac(~5)	187.4 ± 21.2	20.1 ± 1.1	3.8 ± 0.2	12.4 ± 1.2	0.98
D90A-Ac(0) (100 mM NaCl)	150.5 ± 30.9	12.2 ± 1.0	1.5 ± 0.2	9.3 ± 0.9	0.99
D90A-Ac(~2) (100 mM NaCl)	271.6 ± 29.6	18.2 ± 1.3	2.1 ± 0.2	14.0 ± 1.1	0.99
D90A-Ac(~3) (100 mM NaCl)	233.1 ± 21.8	18.5 ± 1.3	2.2 ± 0.2	14.1 ± 1.1	0.98
D90A-Ac(~5) (100 mM NaCl)	160.4 ± 25.6	20.3 ± 1.5	2.6 ± 0.2	15.2 ± 1.4	0.98

TABLE S4 Average kinetic parameters of ThT aggregation assays for acetylated and unacetylated A4V SOD1, in 0 mM and 100 mM NaCl. All data are presented as mean ± SEM, n = 18. The number of acetylated lysine residues is listed per apo-SOD1 monomer.

SOD1	a (maximum) (a.u.)	x_0 (hr)	b (hr)	Lag time (hr)	Average R^2
A4V-Ac(0)	67.4 ± 8.1	18.3 ± 1.8	2.2 ± 0.2	13.8 ± 1.7	0.99
A4V-Ac(~3)	101.6 ± 16	28.2 ± 2.4	4.1 ± 0.4	20.1 ± 2.1	0.99
A4V-Ac(~4)	91.7 ± 8.8	17.8 ± 0.5	3.2 ± 0.3	11.5 ± 0.7	0.99
A4V-Ac(~9)	84.1 ± 13.9	38.0 ± 1.7	4.9 ± 0.3	28.3 ± 1.7	0.99
A4V-Ac(0) (100 mM NaCl)	75.9 ± 6.4	16.9 ± 1.6	2.2 ± 0.3	12.7 ± 1.3	0.98
A4V-Ac(~3) (100 mM NaCl)	169.1 ± 17.4	27.1 ± 1.5	4.8 ± 0.3	17.5 ± 1.3	0.99
A4V-Ac(~4) (100 mM NaCl)	127.2 ± 12.6	24.8 ± 2.4	4.6 ± 0.5	15.6 ± 2.2	0.99
A4V-Ac(~9) (100 mM NaCl)	86.0 ± 16.0	26.6 ± 1.5	4.7 ± 0.4	17.1 ± 1.2	0.99

TABLE S5 Thermostability of native and amyloid WT and ALS-variant apo-SOD1 as a function of lysine acetylation. All of the T_m values are presented as mean ± SEM, n = 4.

SOD1	Ac[a] (~N)	Native T_m (°C)	ΔT_m (°C)[b]	Amyloid T_m (°C)	ΔT_m (°C)[b]
WT	0	52.70 ± 0.05	—	99.42 ± 0.89	—
	1	52.50 ± 0.03	-0.02 ± 0.06	99.64 ± 0.76	-0.22 ± 1.17
	3	50.80 ± 0.03	-1.90 ± 0.06	101.34 ± 0.88	1.92 ± 0.88
	6	46.60 ± 0.03	-6.10 ± 0.06	96.27 ± 0.66	-3.15 ± 1.1
	11	—	—	91.66 ± 0.78	-7.76 ± 1.18
D90A	0	49.70 ± 0.04		104.69 ± 0.24	—
	2	49.10 ± 0.06	-0.60 ± 0.07	100.11 ± 0.97	-4.58 ± 0.99
	3	47.70 ± 0.02	-2.00 ± 0.04	96.02 ± 0.97	-8.67 ± 0.99
	5	46.80 ± 0.04	-2.90 ± 0.04	97.62 ± 0.60	-7.07 ± 0.64
	11	—	—	84.49 ± 0.42	-20.2 ± 0.48
A4V	0	41.10 ± 0.32	—	99.85 ± 0.48	—
	3	39.10 ± 0.36	-2.00 ± 0.48	95.98 ± 1.71	-3.87 ± 1.77
	4	38.70 ± 0.23	-2.40 ± 0.39	92.26 ± 1.31	-7.59 ± 1.39
	9	—	—	95.07 ± 0.33	-4.78 ± 0.58
	11	—	—	95.29 ± 0.50	-4.56 ± 0.69

[a]Mean number of acetylated lysines in apo-SOD1 prior to fibrillization, except Ac(~11), which was acetylated in fibrillar form. Number of acetyl modifications is listed per apo-SOD1 monomer. [b]ΔT_m values for native and amyloid SOD1 are expressed relative to Ac(0) for each protein. All values and errors are listed as mean ± SEM, n = 4.

SUPPORTING REFERENCES

1. Kokot, Z., and K. Burda. 1998. Simultaneous determination of salicylic acid and acetylsalicylic acid in aspirin delayed-release tablet formulations by second-derivative UV spectrophotometry. *J. Pharm. Biomed. Anal.* 18:871-875.
2. Shi, Y., R. A. Mowery, J. Ashley, M. Hentz, A. J. Ramirez, B. Bilgicer, H. Slunt-Brown, D. R. Borchelt, and B. F. Shaw. 2012. Abnormal SDS-PAGE migration of cytosolic proteins can identify domains and mechanisms that control surfactant binding. *Protein Sci.* 21:1197-1209.
3. Shi, Y., N. R. Rhodes, A. Abdolvahabi, T. Kohn, N. P. Cook, A. A. Marti, and B. F. Shaw. 2013. Deamidation of Asparagine to Aspartate Destabilizes Cu, Zn Superoxide Dismutase, Accelerates Fibrillization, and Mirrors ALS-Linked Mutations. *J. Am. Chem. Soc.* 135:15897-15908.
4. Abdolvahabi, A., J. L. Gober, R. A. Mowery, Y. Shi, and B. F. Shaw. 2014. Metal-ion-specific screening of charge effects in protein amide h/d exchange and the hofmeister series. *Anal. Chem.* 86:10303-10310.
5. Erickson, H. P. 2009. Size and shape of protein molecules at the nanometer level determined by sedimentation, gel filtration, and electron microscopy. *Biol. Proced. Online* 11:32-51.
6. Anderson, J. R., O. Chernavskaya, I. Gitlin, G. S. Engel, L. Yuditsky, and G. M. Whitesides. 2002. Analysis by capillary electrophoresis of the kinetics of charge ladder formation for bovine carbonic anhydrase. *Anal. Chem.* 74:1870-1878.
7. Shaw, B. F., A. Durazo, A. M. Nersissian, J. P. Whitelegge, K. F. Faull, and J. S. Valentine. 2006. Local unfolding in a destabilized, pathogenic variant of superoxide dismutase 1 observed with H/D exchange and mass spectrometry. *J. Biol. Chem.* 281:18167-18176.
8. Rodriguez, J. A., B. F. Shaw, A. Durazo, S. H. Sohn, P. A. Doucette, A. M. Nersissian, K. F. Faull, D. K. Eggers, A. Tiwari, L. J. Hayward, and J. S. Valentine. 2005. Destabilization of apoprotein is insufficient to explain Cu,Zn-superoxide dismutase-linked ALS pathogenesis. *Proc. Natl. Acad. Sci. U. S. A.* 102:10516-10521.
9. Furukawa, Y., and T. V. O'Halloran. 2005. Amyotrophic lateral sclerosis mutations have the greatest destabilizing effect on the apo- and reduced form of SOD1, leading to unfolding and oxidative aggregation. *J. Biol. Chem.* 280:17266-17274.
10. Nikolai Lorenzen, E. E. W., and Daniel E. Otzen. 2013. Inhibition of Amyloid Formation by Small Molecules. In Amyloid Fibrils and Prefibrillar Aggregates: Molecular and Biological Properties. D. E. Otzen, editor. Wiley-VCH Verlag & Co. KGaA, Weinheim. 350-356.